**The EMBO Journal** Vol.17 No.13 pp.3726–3737, 1998

# Processing of a dicistronic small nucleolar RNA precursor by the RNA endonuclease Rnt1

**Guillaume Chanfreau[1], Giuseppe Rotondo, Pierre Legrain and Alain Jacquier**

Laboratoire du Métabolisme des ARN, URA1300 CNRS, Institut Pasteur, Departement des Biotechnologies, 25 rue du Dr Roux, F-75724 Paris Cedex 15, France

[1]Corresponding author
e-mail: guillom@pasteur.fr

**Small nucleolar RNAs (snoRNAs) are intron encoded or expressed from monocistronic independent transcription units, or, in the case of plants, from polycistronic clusters. We show that the snR190 and U14 snoRNAs from the yeast *Saccharomyces cerevisiae* are co-transcribed as a dicistronic precursor which is processed by the RNA endonuclease Rnt1, the yeast ortholog of bacterial RNase III. *RNT1* disruption results in a dramatic decrease in the levels of mature U14 and snR190 and in accumulation of dicistronic snR190–U14 RNAs. Addition of recombinant Rnt1 to yeast extracts made from *RNT1* disruptants induces the chase of dicistronic RNAs into mature snoRNAs, showing that dicistronic RNAs correspond to functional precursors stalled in the processing pathway. Rnt1 cleaves a dicistronic transcript *in vitro* in the absence of other factors, separating snR190 from U14. Thus, one of the functions of eukaryotic RNase III is, as for the bacterial enzyme, to liberate monocistronic RNAs from polycistronic transcripts.**

*Keywords*: RNase III/rRNA/snoRNA/snoRNP/U14

## Introduction

Small nucleolar RNAs (snoRNAs) are a class of abundant RNAs found in the nucleolus of eukaryotic cells (reviewed in Bachellerie *et al*., 1995; Maxwell and Fournier, 1995; Smith and Steitz, 1997; Tollervey and Kiss, 1997). Based on the presence of conserved consensus motifs, the snoRNAs have been classified into two families (with the exception of the RNA component of RNase MRP), the box C/D and the box H/ACA families (Balakin *et al*., 1996; Ganot *et al*., 1997b). While some of the snoRNAs are directly required for various cleavages of the pre-rRNA precursor, most of them are implicated in the site-specific modification of nucleotides of the pre-rRNA (reviewed in Tollervey, 1996; Smith and Steitz, 1997; Tollervey and Kiss, 1997). Members of the box C/D family are involved in 2′-*O*-methylation of the pre-rRNA precursor (Cavaille *et al*., 1996; Kiss-Laszlo *et al*., 1996; Tycowski *et al*., 1996b) and members of the box H/ACA family are required for pseudouridylation of the pre-rRNA (Ganot *et al*., 1997a; Ni *et al*., 1997). In both cases, each snoRNA base-pairs with a precise region of the pre-rRNA substrate, acting as a template to specify the site of modification in the pre-rRNA.

The biogenesis pathways of snoRNAs are as fascinating and as diverse as their functions in rRNA processing (reviewed in Bachellerie *et al*., 1995; Maxwell and Fournier, 1995; Smith and Steitz, 1997; Tollervey and Kiss, 1997). This diversity results from the variety of their genomic organization, which differs between distinct phyla of eukaryotes. Most metazoan snoRNAs are encoded within introns of a host gene, which very often encodes a protein involved in translation or ribosome biogenesis (Liu and Maxwell, 1990; Leverette *et al*., 1992; Fragapane *et al*., 1993; Kiss and Filipowicz, 1993; Prislei *et al*., 1993; Tycowski *et al*., 1993, 1996a). While most of these metazoan intron-encoded snoRNAs are processed by exonucleolytic processing of the pre-mRNA or of the excised intron (Leverette *et al*., 1992; Tycowski *et al*., 1993; Kiss and Filipowicz, 1995), some others require endonucleolytic cleavage of the pre-mRNA prior to exonucleolytic trimming up to the mature ends (Caffarelli *et al*., 1994). In plants, snoRNAs are encoded in polycistronic clusters (Leader *et al*., 1994, 1997). Proper processing to the mature forms requires endonucleolytic cleavage (Leader *et al*., 1997). The situation in the yeast *Saccharomyces cerevisiae* is mixed. Some snoRNAs are transcribed independently, while some others are intron encoded (reviewed in Maxwell and Fournier, 1995; Tollervey and Kiss, 1997). In the latter case, processing to the mature form involves debranching to the excised intron and exonucleolytic processing to the mature snoRNAs by the Rat1 and the Xrn1 exonucleases (Petfalski *et al*., 1998).

U14 snoRNA constitutes a paradigm for the study of snoRNA biosynthesis in yeast and has been the object of intense investigations over the past years. U14 is essential in yeast (Zagorski *et al*., 1988) and is required for 18S rRNA production (Li *et al*., 1990). The lack of cap at the 5′ end of U14 as well as the heterogeneity of the U14 ends (Balakin *et al*., 1994) have suggested that U14 is processed post-transcriptionally. Extensive mutagenesis studies have shown that the box C and D sequences, as well as a terminal stem–loop joining the 5′ and 3′ boundaries of the RNA are required for proper expression of U14 (Huang *et al*., 1992). The importance of boxes C and D for snoRNA biosynthesis and stability has also been demonstrated for mouse U14 (Watkins *et al*., 1996; Xia *et al*., 1997) and for other vertebrate box C/D snoRNAs (Caffarelli *et al*., 1996), showing that yeast U14 constitutes a valid model for studying snoRNA biogenesis. In contrast to its mammalian ortholog, yeast U14 is not intron encoded (Zagorski *et al*., 1988). However, its genomic architecture is peculiar since the U14 coding sequence is located only 67 nucleotides downstream from another box C/D snoRNA, snR190 (Zagorski *et al*., 1988). The lack of

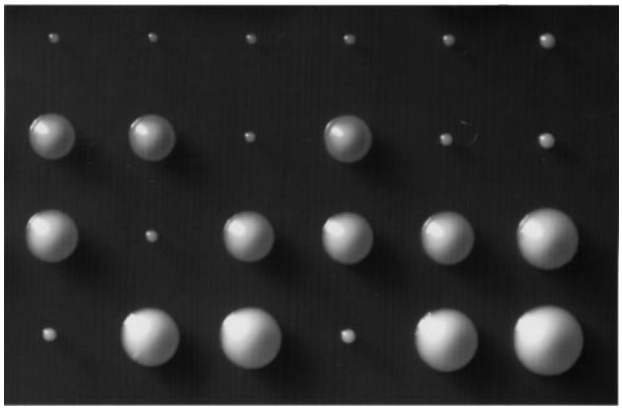

**Fig. 1.** Tetrad analysis of *RNT1*/*rnt1*::*TRP1* heterozygotes. Tetrads were dissected on a YPD plate, which was incubated for 6 days at 24°C. Six dissected tetrads are shown. Nineteen tetrads were dissected from two independent diploids, which all showed the same segregation. The spores with a slow growth phenotype were all prototrophic for tryptophan, while the spores with a normal growth were all auxotrophic for tryptophan.

obvious promoter sequence between the snR190 and U14 coding sequences (Zagorski *et al*., 1988) and the existence of small amounts of RNAs hybridizing to both U14 and snR190 probes in *rat1, xrn1* exonuclease mutants (Petfalski *et al*., 1998) have suggested that the biogenesis of these two RNAs involves co-expression in a single transcript, followed by processing.

The *RNT1* gene encodes the *S.cerevisiae* ortholog of bacterial RNase III (Abou Elela *et al*., 1996). Rnt1 possesses double-stranded RNA endonuclease activity and has been shown to process the precursor of rRNA as well as the spliceosomal U5 and U2 snRNAs (Abou Elela *et al*., 1996; Chanfreau *et al*., 1997; Abou Elela and Ares, 1998). In this study, we show that *RNT1* disruption results in a severe growth defect and in a dramatic decrease in the *in vivo* levels of U14 and snR190 snoRNAs. We show that Rnt1 is involved in the processing of these snoRNAs and that it cleaves a dicistronic snR190–U14 precursor, separating snR190 from U14. These results indicate that, like the prokaryotic enzyme, eukaryotic RNase III can process polycistronic RNAs to generate individual transcripts.

## Results

### *Disruption of the RNT1 gene is not lethal but results in a serious growth defect*

The *RNT1* gene has been described as essential for yeast vegetative growth (Abou Elela *et al*., 1996). During an earlier study (Chanfreau *et al*., 1997), we noticed that the disrupted strain complemented by a plasmid-borne version of the *RNT1* gene could lose the complementing plasmid, yielding cells with a severe growth defect and a temperature-sensitive phenotype. Because the initial knockout of the gene was performed by insertion of a *HIS3* marker in the middle of the *RNT1* open reading frame (ORF) (Abou Elela *et al*., 1996) and because this disruption retained the possibility of expression of a truncated Rnt1 fusion protein (Chanfreau *et al*., 1997), we re-examined the effect of a complete deletion of the gene by replacing the whole *RNT1* ORF precisely with the *TRP1* auxotrophy marker (see Materials and methods). Tetrad dissection (Figure 1) revealed that disruption of the *RNT1* gene results in a severe growth defect, the generation time of the cells lacking *RNT1* (*rnt1*Δ) ranging between 7 and 9 h at 30°C in glucose complete medium (YPD). The growth defect was exacerbated at 37°C (data not shown) but not by incubation at 15°C, nor on glycerol or galactose medium. The growth defect could be complemented by a centromeric plasmid-borne version of the *RNT1* gene (data not shown). Similar results have been obtained with a different *RNT1* deletion knockout (Abou Elela and Ares, 1998). We conclude that disruption of *RNT1* is not lethal in *S.cerevisiae* but results in a severe growth defect. This result is reminiscent of the situation in *Escherichia coli*, where disruption of the *rnc* gene encoding RNase III results in viable, albeit slow-growing cells (Takiff *et al*., 1989; see Discussion).

### *Biogenesis of U14 and snR190 transcripts is severely affected in rnt1Δ cells*

Rnt1 previously was shown to be involved in the biogenesis of the spliceosomal U5 snRNA (Chanfreau *et al*., 1997). The availability of cells which are viable but disrupted for *RNT1* allowed us to screen for other RNAs whose levels are changed in the absence of Rnt1. To this end, total RNAs were extracted from a tetrad of four isogenic sister spores (two wild-type and two *RNT1*-disrupted sister spores) and the level of RNAs was assessed by Northern blot using $^{32}$P-5′-labeled oligonucleotide probes (Figure 2A). A screen for snoRNAs affected by the disruption of *RNT1* revealed a dramatic decrease in the level of mature U14 snoRNA in the *rnt1*Δ spores, as compared with the isogenic wild-type sister spores (Figure 2B; a low level of mature U14 could, however, be detected on overexposed gels in *rnt1*Δ RNAs; data not shown and see below). The snR3 snoRNA was used as a standard because its level is not changed significantly by *RNT1* disruption (Figure 2B). In contrast to the lack of mature U14, the U14 probe detected in the *rnt1*Δ RNAs a major species of 540 nucleotides (named UMO1 on Figure 2B for unidentified migrating object 1), as well as a less abundant species of 385 nucleotides, named UMO2. The fact that the genes encoding U14 and snR190 are separated by only 67 nucleotides (Zagorski *et al*., 1988; Figure 2A) raised the possibility that some of these *rnt1*Δ-specific RNAs are dicistronic snR190–U14 transcripts. Thus, we next examined the levels of the snR190 snoRNA in the *rnt1*Δ cells. A strong decrease in the steady-state level of snR190 was observed in *rnt1*Δ RNAs, with an accumulation of the UMO1 and UMO2 species previously detected with the U14 probe (Figure 2B). In addition to these products, the snR190 probe detected an additional abundant species of 340 nucleotides, named UMO3. To investigate further the organization of the *rnt1*Δ-specific RNAs, we probed the same membrane with a probe complementary to a part of the intergenic region which separates the two coding sequences (ITS probe, Figure 2A). This probe did not detect any product in wild-type cells but detected the UMO1 and UMO2 species in the RNAs extracted from the *rnt1*Δ cells (Figure 2B). A probe hybridizing to a sequence upstream from snR190 (UPS probe, Figure 2A) detected only the UMO1 and UMO3 products, and that exclusively in the sample from the *RNT1*-disrupted cells (Figure 2B). Taken together, these

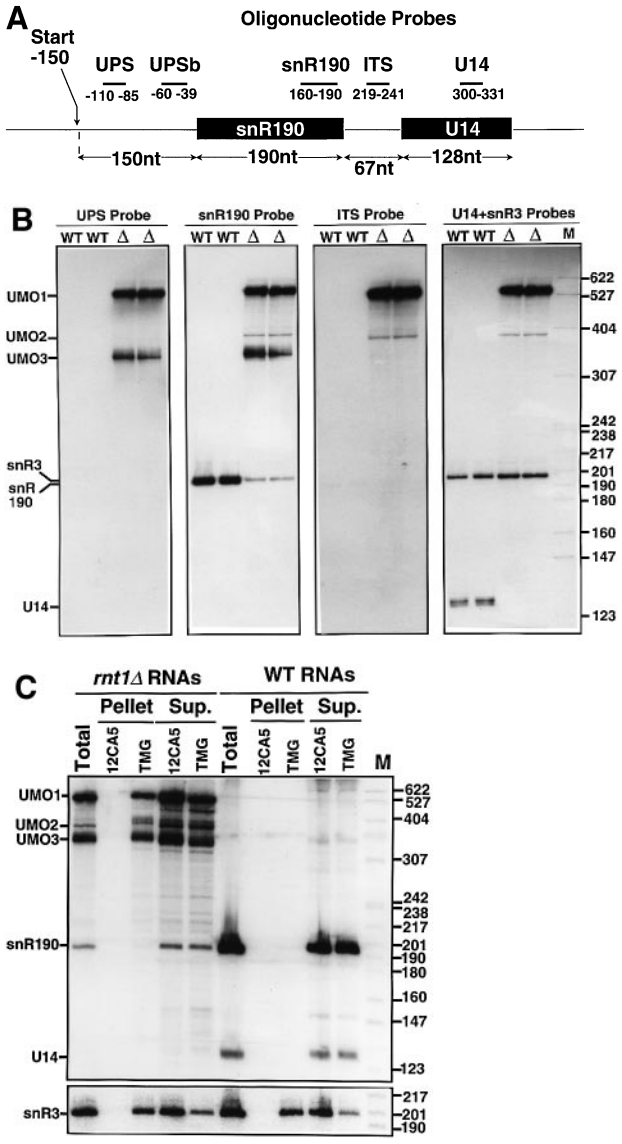


**Fig. 2.** Biogenesis of the snR190 and U14 snoRNAs in wild-type and *RNT1*-disrupted cells. (**A**) Organization of the snR190–U14 genomic region and oligonucleotide probes used for the mapping of the aberrant species. The position of the oligonucleotide probes is indicated taking the beginning of the snR190 coding sequence as the origin. (**B**) Northern blot analysis of the RNAs extracted from two wild-type spores (WT) and two spores disrupted for RNT1 (Δ). The membrane was hybridized successively with the U14 and snR3 probes, the snR190 probe, the intergenic probe and the upstream probe. The molecular weight marker is pBR322 digested with *Msp*I (Biolabs) and labeled with [$\gamma$-$^{32}$P]ATP by phosphate exchange reaction. The positions of U14, snR190, snR3, UMO1, UMO2 and UMO3 are indicated on the left. The only band detected by the snR3 probe was the mature snR3; all the other bands are due to hybridization with the U14 probe. (**C**) Immunoprecipitations of TMG-capped species in wild-type and *rnt1*Δ RNAs. Shown is a Northern blot probed for snR3 (bottom panel) or for snR190 and U14 (top panel). Total indicates the total amount of wild-type or *rnt1*Δ RNAs used in the immunoprecipitation reactions. Pellets indicate the RNAs retained on beads coupled to the control 12CA5 antibody (12CA5) or to the anti-TMG antibody. Supernatant (Sup.) corresponds to the RNAs present in the supernatant prior to the first wash. M is the pBR322/*Msp*I molecular weight marker.

results indicate that: (i) the UMO1 contains sequences upstream from the snR190 coding sequence, sequences from the U14 and snR190 snoRNAs as well as from the 67 nucleotide spacer; (ii) the UMO2 contain sequences from the U14 and snR190 snoRNAs and from the 67 nucleotide spacer; and (iii) the UMO3 species contains sequences upstream from and within the snR190 coding sequence, but does not hybridize either with the U14 probe or with the intergenic spacer probe. All the phenotypes observed in the *rnt1*Δ cells could be suppressed by a plasmid-borne version of the *RNT1* gene (data not shown).

### *Some of the rnt1Δ-specific transcripts possess a trimethylguanosine cap*

The steady-state levels of the UMO1 and UMO3 species, which are equivalent to the steady-state level of snR190 in the wild-type samples (Figure 2B), indicate that these species are very stable. One explanation for this stability might be that they are protected at their 5′ end by a trimethylguanosine (TMG) cap. To test whether these species are TMG-capped, we performed immunoprecipitation of total RNAs from the wild-type or the *rnt1*Δ strains with the K121 mouse monoclonal antibody directed against the TMG cap (Krainer, 1988; Figure 2C; Materials and methods). The 12CA5 monoclonal antibody was used as a negative control because it is a mouse monoclonal antibody of the same subclass ($IgG_1$). After immunoprecipitation, RNAs were fractionated on a polyacrylamide gel and revealed by Northern blot. To provide a positive control for the immunoprecipitation, the blot was probed for snR3 which possess a TMG cap. Figure 2C shows that this snoRNA was immunoprecipitated efficiently by the anti-TMG antibody, but not by the control antibody, in both wild-type and *rnt1*Δ samples. The same blot was then probed with the U14 and snR190 oligonucleotide probes (Figure 2C). The UMO1 and UMO3 RNAs from the *rnt1*Δ strain were immunoprecipitated efficiently by the anti-TMG antibody, but not by the control antibody. In contrast, the UMO2 RNA was not immunoprecipitated. We do not think that the band migrating slightly above UMO2 in the immunoprecipitate lane is actually UMO2, because the corresponding supernatant lane does not show any depletion of UMO2, while in the same lane, UMO1 and UMO3 are significantly depleted in the supernatant. Mature snR190 and U14 snoRNAs were not immunoprecipitated, consistent with their lack of cap (Balakin *et al*., 1994). This experiment demonstrates that the UMO1 and UMO3 RNAs possess a TMG cap which could partially explain their stability *in vivo*.

### *Mapping of the rnt1Δ-specific transcripts*

We undertook further characterization of the two most abundant, TMG-capped species found in the *rnt1*Δ cells, the UMO1 and UMO3 RNAs. To investigate the topology of these species and to check that neither of them arises from aberrant splicing or genomic rearrangements, we performed RNase protection using radiolabeled antisense probes spanning the whole snR190–U14 genomic region. These probes gave rise to protected bands of the same size as snR190 and U14 snoRNAs in RNAs from the wild-type cells, and of the same size as the UMOs species from the *rnt1*Δ cells (data not shown), indicating that the UMOs are co-linear with the DNA sequence and that they do not arise from a splicing or a genomic rearrangement event.

The 5′ ends of the UMO1 and UMO3 species present

in the *rnt1*Δ cells were mapped by primer extension. Primer extension with various oligonucleotides staggered over the snR190–U14 genomic region (U14, snR190 and ITS primers; Figure 2A) yielded for each primer a single major cDNA in the *rnt1*Δ samples (Figure 3A; the primer extension stop seen at the level of the mature snR190 is probably a mixture of stops derived from the low level of mature snR190 and of UMO2). The more downstream the primer, the longer the cDNA, consistent with a single major 5′ end for both UMO1 and UMO3. This 5′ end was determined precisely using primer extension with oligonucleotide UPSb (Figure 2A), in parallel with a sequencing ladder obtained with the same 5′-labeled primer (Figure 3B). The 5′ end was heterogenous, the major stop of reverse transcription being located 150 nucleotides from the 5′ end of the snR190. Since these 5′ ends possess a TMG cap (Figure 2C), and since the presence of a cap is indicative of the start of transcription, this heterogeneity probably reflects multiple starts of transcription.

Because the last probe to which the UMO1 RNAs hybridizes is complementary to U14 (Figure 2B), the 3′ end of the UMO1 was determined by RNase A/T1 mapping using two antisense RNA probes: probe A starts at the 5′ end of U14 and ends 136 nucleotides downstream from the 3′ end of U14, and probe B starts 50 nucleotides upstream from U14 and ends at the same site as probe A (Figure 3C; polylinker sequences are not shown on the diagram). Digestion of probe A showed that the RNAs from the wild-type and the *rnt1*Δ cells which contain a U14 sequence have the same 3′ end, and that none of the *rnt1*Δ-specific species has longer 3′ ends than mature U14 (Figure 3C). When probe B was used, species longer on the 5′ side were detected in the *rnt1*Δ sample, but no protected band corresponding to mature U14 was detected in this sample (Figure 3C), showing that the signal generated with probe A in *rnt1*Δ RNAs was not due to the low level of mature U14. The 3′ end of the UMO3 was not mapped by RNase mapping. However, this RNA hybridizes with a probe located at the 3′ end of snR190, which is 190 nucleotides long. We have mapped the 5′ end of the UMO3 150 nucleotides away from the 5′ end of snR190. Given that the UMO3 is 340 nucleotides long (equal to the sum of 190 and 150), it is likely to end at the mature 3′ end of snR190 or close to it. Consistent with this hypothesis, the UMO3 RNA does not hybridize with the ITS probe (Figure 2B).

The results of the mapping of the UMOs by Northern blot, primer extension and RNase mapping suggest the organization of the *rnt1*Δ-specific RNAs summarized in Figure 3D. The UMO1 species contains 150 nucleotides upstream of snR190, the snR190 sequence, the intergenic spacer and the U14 sequence. It is TMG-capped and its 3′ end corresponds to the 3′ end of mature U14. Concerning the UMO2, we have not mapped its boundaries precisely. However, its size, combined with the fact that it hybridizes to the probes complementary to snR190 and U14, as well as to the ITS probe, suggests that it begins at the 5′ end of snR190 and ends at the 3′ end of U14 (Figure 3D). The UMO3 is TMG-capped and contains 150 nucleotides upstream of snR190, the snR190 sequence and probably ends at the mature 3′ end of snR190 or close to it (Figure 3D). The 5′ ends of the UMO1 and UMO3 RNAs are identical and indicative of the actual site of transcription initiation because of the cap structure present (Figure 2C).

### *Addition of Rnt1 to rnt1Δ extracts chases the endogenous dicistronic transcripts into mature U14 and snR190*

The organization of the *rnt1*Δ-specific RNAs suggested that the snR190 and U14 snoRNAs are co-transcribed as a single dicistronic precursor and that cleavage by Rnt1 is required at some step of the processing pathway; in its absence, unprocessed or partially processed species accumulate. Alternatively, these RNAs may correspond to dead-end products accumulating in the context of the disruption of *RNT1* because their decay requires Rnt1. If these species are not dead-end products but are stalled in the processing pathway at a step requiring Rnt1, one would expect that addition of recombinant Rnt1 to whole-cell extracts made from *rnt1*Δ cells would chase the endogenous dicistronic RNAs into mature RNAs. To test this hypothesis, whole-cell extracts were prepared from isogenic wild-type and *RNT1*-disrupted sister spores and the *rnt1*Δ extract was incubated in processing conditions with buffer only, purified recombinant glutathione-*S*-transferase–Rnt1 (GST–Rnt1) or with GST alone. After incubation, the endogenous RNAs present in the whole-cell extracts were examined by Northern blot with snR190 and U14 oligonucleotide probes. As shown in Figure 4, incubation of the *rnt1*Δ extract with recombinant GST–Rnt1 resulted in the chase of the endogenous dicistronic UMO1 RNA into mature snR190 and U14 snoRNAs. Quantitation of the RNA levels showed that most of the mature U14 and snR190 snoRNAs generated by the chase were due to conversion of the UMO1 RNA. The final level of the mature U14 and snR190 after the chase was close to the level observed in the wild-type extract (Figure 4). The levels of UMO2 and UMO3 also decreased upon incubation with GST–Rnt1. However, we think that this decrease is not due to cleavage by GST–Rnt1 *per se*, but rather to degradation of these two species by endogenous nucleases present in the extract. This effect is masked in the control lanes (buffer and GST) because conversion of UMO1 into UMO2 and UMO3 compensates for the degradation of those species, resulting in an apparent increase in UMO2 and only a slight decrease in UMO3. In these conditions, some enhancement of the levels of the mature snR190 or U14 and of the UMO2 RNA was also observed. This effect probably is due to the endogenous nucleases present in the yeast whole-cell extract, which are activated by the magnesium contained in the buffer and can partially degrade the UMO1 and UMO3 RNAs, converting them into mature snoRNAs or into UMO2. Finally, incubation of the wild-type extract with buffer, GST or GST–Rnt1 did not result in any significant change (data not shown). This experiment demonstrates that the UMO1 dicistronic RNAs observed in *rnt1*Δ cells does not correspond to a dead-end product and that it can be chased into mature RNAs by addition of Rnt1. No obvious intermediates were observed, indicating that Rnt1 cleavage is a rate-limiting step, *in vitro* as *in vivo* (Figure 2).

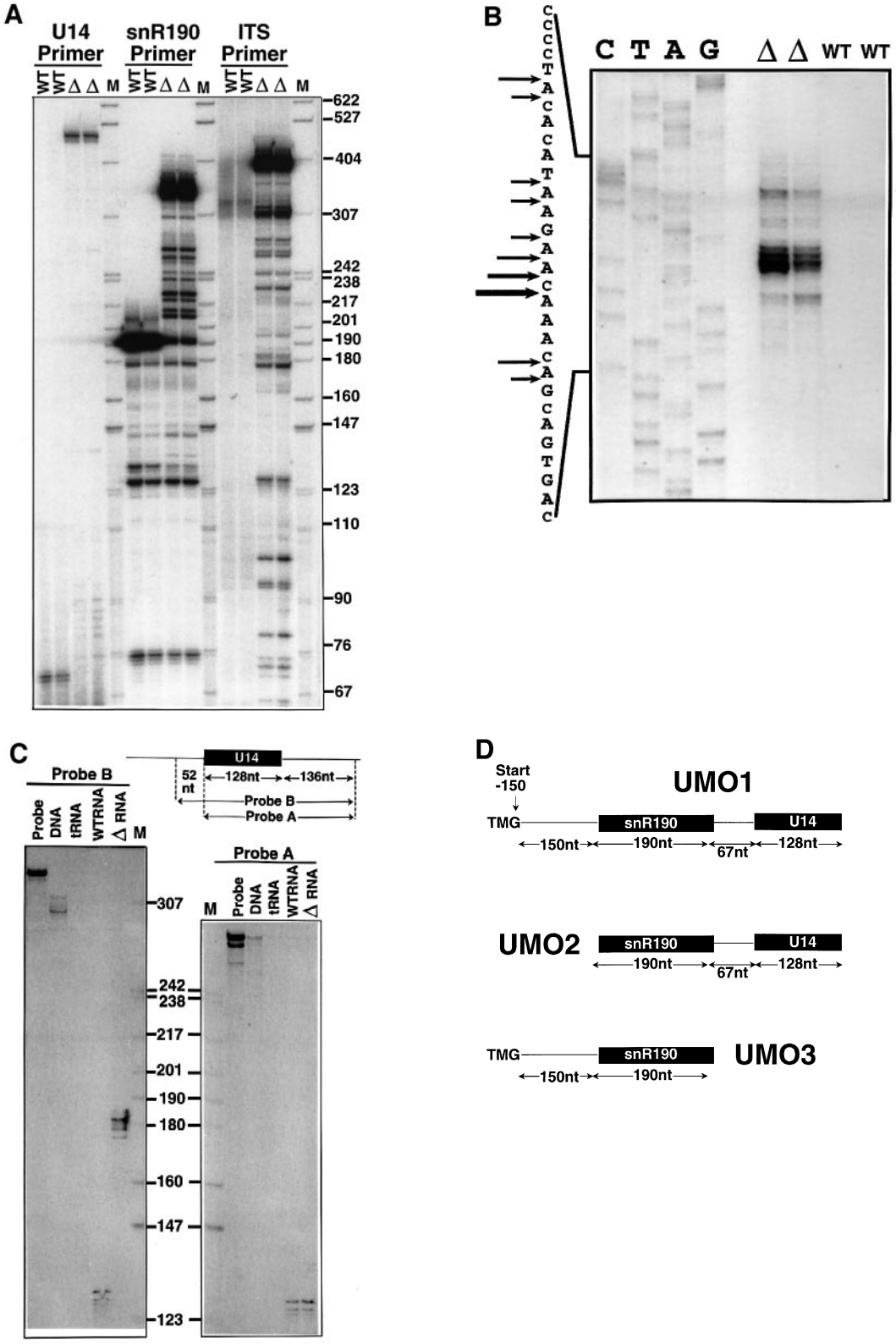


**Fig. 3.** Molecular mapping of the RNAs found in the *rnt1*Δ cells. (**A**) Primer extension analysis with U14, snR190 and ITS primers. Primer extension was done with RNAs from the two wild-type spores (WT) and RNAs from the *RNT1*-disrupted sister spores (Δ). (**B**) Primer extension analysis with the UPSb primer. The 5′ ends are indicated by arrows on the sequence on the left. The length and thickness of the arrows are roughly proportional to the intensities of reverse transcriptase stops. No products were observed for the WT RNAs in other portions of the gel. (**C**) RNase A/T1 mapping of the 3′ ends of the UMO1 species. Shown is the organization of probes A and B, with the result of the digestion of these probes after hybridization with plasmid DNA (10 ng), tRNA (5 μg) or 2–4 μg of total RNAs from WT or *rnt1*Δ cells. Undigested probe corresponding to 1/10 of the amount of probe annealed to the different samples is loaded on the first lane. The RNA probes also contain at their 5′ end polylinker sequences from pSP64 and at their 3′ end the reverse complement of the T7 polymerase promoter, which are not shown on the diagram of the probes. (**D**) Schematic organization of the RNA species found in the *rnt1*Δ cells.

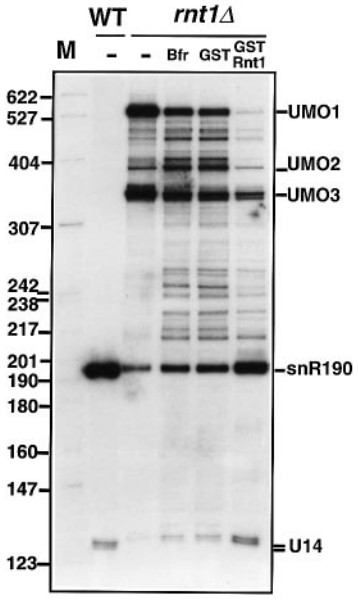


**Fig. 4.** Addition of recombinant Rnt1 to extracts from *rnt1*Δ cells results in the chase of the endogenous dicistronic precursor into mature snR190 and U14. Northern blot of the endogenous RNAs found in whole-cell extracts from wild-type cells (WT) or *rnt1*Δ cells with no incubation (– lane) or after 45 min of incubation with buffer alone, with GST or with GST–Rnt1. The blot was probed simultaneously with snR190 and U14 probes. Note that U14 is heterogeneous in size, as previously reported (Balakin *et al*., 1994). The small amount of mature U14 observed in the *rnt1*Δ extracts was observed reproducibly to be 1–2 nucleotides longer than the U14 from WT cells. The basis of this difference is not known.

### *Recombinant Rnt1 cleaves a model precursor transcript in vitro in the absence of other factors*

The ability of recombinant Rnt1 to chase the endogenous dicistronic RNAs into mature U14 and snR190 in *rnt1*Δ extracts, and the accumulation of 5′-extended forms of U14 and snR190 in the *rat1* and *xrn1* exonuclease mutants (Petfalski *et al*., 1998) suggest a pathway in which the dicistronic RNAs are first cleaved by Rnt1 and then processed to the mature ends by exonucleases which are present in the extract. To investigate the ability of Rnt1 to cleave the snR190–U14 transcript directly, we incubated a model dicistronic radiolabeled transcript generated by *in vitro* transcription with purified GST–Rnt1 or with GST or buffer alone (Figure 5A). Incubation of this transcript with GST–Rnt1 yielded three major fragments (labeled A, B and C in Figure 5A), which are not observed upon incubation with buffer or GST alone. These fragments are likely to be due specifically to cleavage by Rnt1 because the same cleavage pattern was observed when the same transcript was incubated in wild-type whole-cell extracts, but not in extracts made from *rnt1*Δ cells (Figure 5). Other minor fragments were observed (Figure 5A). However, given their weak intensity and that they were not observed upon incubation with the wild-type extract, they correspond to minor cleavage events. Thus they were not analyzed further. The sum of the approximate sizes of the three major fragments A, B and C (280 + 245 + 50) is approximately equal to the size of the full-length precursor (570), consistent with a double cleavage event by Rnt1. The three major fragments generated by Rnt1 cleavage were gel purified and mapped by RNase H digestion using oligonucleotides UPSb, snR190, ITS and U14 (Figures 2A and 5B). Cleavage of a fragment in the presence of a given oligonucleotide indicates that this oligonucleotide can hybridize to the fragment, allowing a rapid mapping of the different cleavage fragment. RNase H mapping showed that fragment A corresponds to the 3′ fragment containing U14 and part of the intergenic region. Fragment B corresponds to the internal fragment containing snR190 and the remaining part of the internal spacer (which does not hybridize to the ITS oligonucleotide). Fragment C corresponds to the fragment upstream from snR190. Note that fragments B and C were both digested with oligo UPSb, suggesting that this oligonucleotide spans one of the cleavage sites. These results show that Rnt1 cleavage liberates RNA fragments corresponding to snR190 and U14 with 5′ and 3′ extensions. Because no processing to the mature ends was observed upon incubation with recombinant Rnt1 alone, we conclude that processing to the mature ends requires other enzymes, presumably exonucleases (Petfalski *et al*., 1998).

The cleavage sites were mapped by primer extension with reverse transcriptase on the products of the *in vitro* cleavage reaction (Figure 6A) and are indicated in Figure 6B which shows the potential secondary structure of the model dicistronic transcript used in this study (established by RNA folding using MFold; Zuker, 1994; see Figure 6 legend). The two Rnt1 cleavage sites are located on opposite sides in the same potential double-stranded region, in agreement with the properties described for RNase III-like enzymes (Chelladurai *et al*., 1993; Court, 1993; Zhang and Nicholson, 1997; see Discussion). It is significant that the 5′ extensions generated by Rnt1 cleavage are identical to the 5′ extensions of snR190 and U14 which have been mapped in yeast strains mutants for two exonucleases (Petfalski *et al*., 1998).

## Discussion

We have shown that in yeast cells disrupted for the yeast ortholog of RNase III (*RNT1*), the biosynthesis of the snR190 and U14 snoRNAs is severely affected. The steady-state levels of U14 and snR190 snoRNAs are dramatically decreased, and species corresponding to unprocessed or partially processed dicistronic snR190–U14 snoRNA transcripts accumulate. Rnt1 is able to cleave a discistronic precursor, liberating monocistronic RNAs. These data indicate that the snR190 and U14 snoRNAs are expressed as a functional dicistronic RNA whose processing requires Rnt1.

### *RNT1: essential or not essential?*

*RNT1* was first described as essential by Abou Elela *et al*. (1996), who assayed the viability of spores at 30°C after tetrad dissection. During an earlier study, we found that cells disrupted for *RNT1* by insertion of an auxotrophy marker could lose the complementing wild-type plasmid, leading to cells with a slow-growing phenotype (Chanfreau *et al*., 1997). This observation raised some doubts about whether *RNT1* is strictly required for cell life. We have now deleted the *RNT1* ORF precisely and we show that the complete disruption leads to viable, albeit seriously sick yeast cells after tetrad dissection at 24°C (Figure 1). Similar results have been obtained with a different *RNT1*

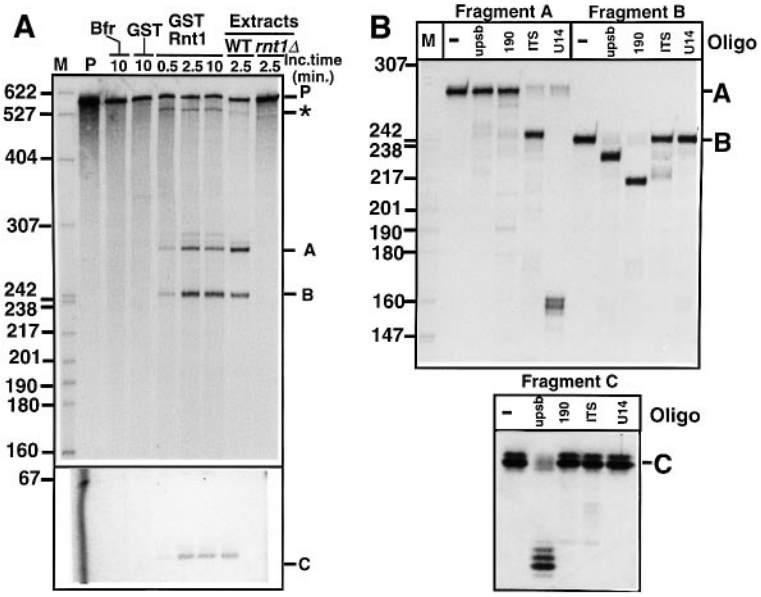


**Fig. 5.** *In vitro* cleavage of a model dicistronic pre-snR190–U14 transcript by Rnt1 liberates snR190 from U14. (**A**) *In vitro* cleavage. Shown are the position of the precursor (P), and of the cleavage fragments A, B and C. The asterisk points to a minor cleavage event which has not been analyzed further. The model precursor contains 92 nucleotides upstream from snR190; the snR190 and U14 sequences are separated by the 67 nucleotide spacer and 95 nucleotides of sequence downstream from U14 (see also Figure 6B). No cleavage fragments were observed on the portion of the gel which is not shown. Because of the weak labeling of the smaller cleavage fragment C, the portion of the gel showing this fragment was taken from an exposure different from that in the upper part of the gel. (**B**) RNase H mapping of the cleavage fragments. Gel-purified fragments A, B and C were incubated with RNase H and the corresponding oligonucleotides as described in Materials and methods. For each fragment, the first lane (–) corresponds to undigested fragment.

deletion knockout (Abou Elela and Ares, 1998). Therefore, it seems likely that *RNT1* is not strictly required for yeast growth, but its absence seriously debilitates cell fitness. This is similar to the situation in prokaryotes, where RNase III disruption is not lethal (Takiff *et al*., 1989). In both organisms, this dispensability may be explained by the notion that RNA processing and degradation pathways are very often redundant and that the essential functions of RNase III can be partially fulfilled by some exonucleases or other endonucleases. This idea has been illustrated for Rnt1 in the case of U5 snRNA 3′ end processing (Chanfreau *et al*., 1997) and for another endonuclease activity in the case of yeast tRNA 3′ end processing (see Yoo and Wolin, 1997).

### *A novel cleavage site for the yeast ortholog of RNase III*

Rnt1 is a double-stranded RNA endonuclease which has been shown to cut the precursor of rRNA at two sites (Abou Elela *et al*., 1996), as well as the precursors of the U5 and U2 snRNAs (Chanfreau *et al*., 1997; Abou Elela and Ares, 1998). The identification of a novel cleavage site within the dicistronic snR190–U14 snoRNA leads to a total of five known targets for this endonuclease. In all cases, the Rnt1 endonuclease cleaves in a double-stranded RNA region. While there seems to be a minimum length of the stem for cleavage, there is no strong sequence identity between the various cleavage sites identified for this enzyme. Thus, the intringuing question arises of what distinguishes the target sites from other double-stranded regions? The answer possibly will come from prokaryotes, where it has been shown that the specificity of the cleavage of the bacterial enzyme relies on sequence anti-determinants: good substrates for RNase III exclude some Watson–Crick base pairs at defined positions relative to the cleavage site (Zhang and Nicholson, 1997). The U5 and the snR190–U14 'eukaryotic' cleavage sites also obey these anti-determinants rules, and it is possible that the prokaryotic and the eukaryotic enzymes share some of these specificity rules. Whatever these similarities, our results also provide an interesting example of functional convergence between the bacterial and the eukaryotic enzymes, since both enzymes process polycistronic transcripts to generate individual RNAs (for review, see Court, 1993).

### *Multiple control of rRNA processing by RNA processing enzymes*

Our results show that Rnt1 controls the biogenesis of U14, a snoRNA which has been implicated in the processing of rRNA. Genetic depletion of U14 has shown that this snoRNA is involved in the cleavage at site A1 within the 5′ external transcribed spacer (ETS) (Li *et al*., 1990), and elegant compensatory mutation analysis (Liang and Fournier, 1995) as well as cross-linking data (Morrissey and Tollervey, 1997) have indicated that this snoRNA interacts with the pre-rRNA. Thus, Rnt1 controls rRNA processing in two ways: directly, by cleaving the pre-rRNA precursor, and indirectly by controlling the steady-state level of one of the components essential for rRNA maturation. This situation is also found in the case of the Xrn1 and Rat1 exonucleases, which are required for processing of both 5.8S rRNA and the snR190 and U14 snoRNAs (Dichtl *et al*., 1997; Petfalski *et al*., 1998). Hence, an emergent concept of double control of rRNA processing by RNA processing enzymes is suggested by

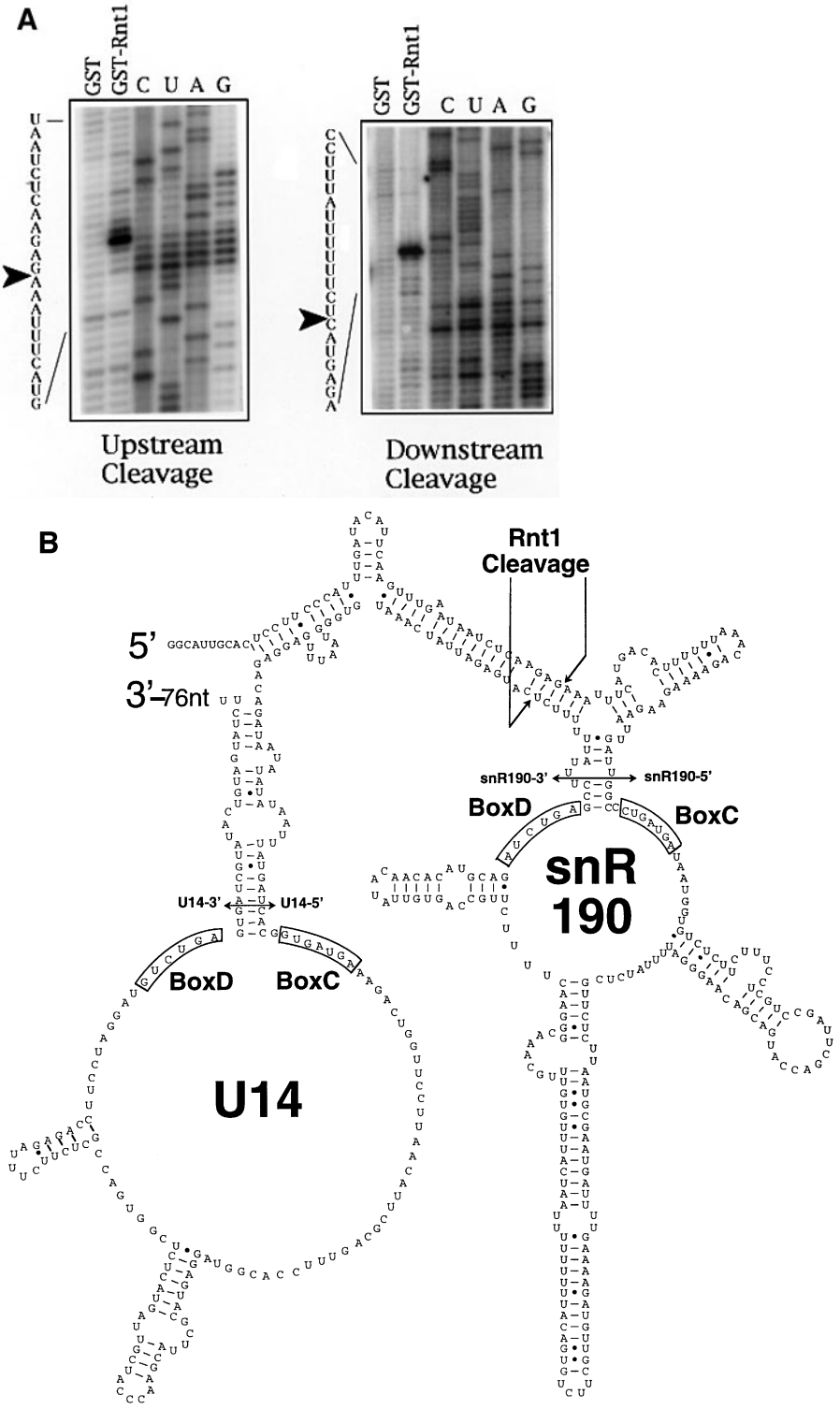


**Fig. 6.** Cleavage sites of Rnt1 in the dicistronic precursor transcript. (**A**) Identification of cleavage sites by primer extension with reverse transcriptase. Primer extension was performed on RNA which was incubated for 15 min at 23°C with GST (RNA+GST) or with GST–Rnt1 (RNA+GST–Rnt1). A reverse transcriptase stop present in the GST–Rnt1 lane but not in the GST lane is indicative of an Rnt1cleavage site. A sequencing ladder was obtained with the same primer, as described in Materials and methods. Shown are the portions of the sequencing gels indicative of the upstream and downstream cleavage sites. The sequencing ladder near the upstream cleavage site fell into an area of strong stops by the polymerase. However, determination of the cleavage site was possible because the number of stops was identical to the number of bases on the sequence. Cleavage sites are indicated by arrowheads on the sequences. The upstream cleavage site was mapped using oligonucleotide Seq190, while the downstream cleavage site was mapped using oligonucleotide U14. (**B**) Localization of cleavage sites in the dicistronic transcript. A potential secondary structure was established by keeping structures which are always present in each of the four most stable structures calculated with MFold (Zuker, 1994). The stem in which Rnt1 cleaves is present in all the most stable secondary structures. The snR190 snoRNA does not exhibit a strong potential structure using MFold. Therefore, a structure was chosen arbitrarily that keeps intact a 5′–3′ terminal stem. U14 secondary structure was drawn from Balakin *et al*. (1994). The 3′ part of the precursor is not shown and does not display a well-conserved potential secondary structure. U14 and snR190 boundaries are indicated by double arrows. Conserved boxes C and D are boxed.

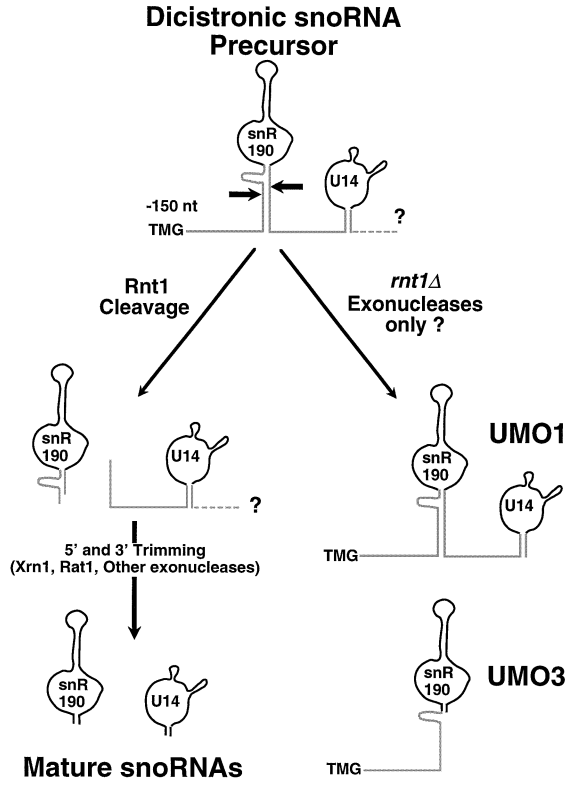


**Fig. 7.** A possible pathway for the biogenesis of snR190 and U14 snoRNAs from dicistronic precursors. The thick arrows represent Rnt1 cleavage. Shown is the pathway in the wild-type cells, and the exonucleolytic pathway that leads to the main UMO RNAs in the *rnt1*Δ cells (the UMO2 RNA is not shown). Gray lines represent sequences which are not found in the mature snoRNAs. The question mark at the 3′ end of the dicistronic precursor symbolizes the fact that the actual 3′ end of the dicistronic precursor is unknown.

our study and work from Tollervey and co-workers. This double control possibly has been selected during evolution to coordinate direct processing of the rRNA and the synthesis of other components required for rRNA biogenesis. While this is an interesting example of control of multiple RNA processing pathways by the same RNase, it also constitutes a potential caveat for studying *in vivo* the role of RNA nucleases in rRNA processing. We do not know if the dicistronic snR190–U14 RNAs observed in *rnt1*Δ cells retain any of the functional properties of the mature U14 required for rRNA processing. Therefore, care should be taken in interpreting the decrease in the steady-state levels of rRNA observed in *RNT1* mutant strains (Abou Elela *et al*., 1996). Whether the rate-limiting step in rRNA processing in mutant cells is the direct cleavage at A0 and at the 3′ ETS, the U14-dependent cleavage at A1, or a combination of both, remains to be elucidated.

### *A pathway for the biogenesis of snR190 and U14 snoRNAs*

The experiments described above suggest a pathway for the processing of snR190 and U14 mature snoRNAs from a single dicistronic snR190–U14 precursor bearing 5′ and 3′ extensions (Figure 7). It is likely that the common 5′ extensions of the UMO1 and UMO3 RNAs are indicative of the transcriptional start site, since this common extension possesses a hypermethylated cap at its 5′ end. The existence of a 3′ extension downstream from U14 has been postulated, because it would extend the terminal stem joining the 5′ and the 3′ ends of U14 (Huang *et al*., 1992; Balakin *et al*., 1994; see Figure 6), but its existence has not yet been proven. Cleavage by Rnt1 is an early step in the processing pathway and is required for efficient production of mature snoRNAs, *in vivo* (Figure 2) as *in vitro* (Figure 4). Its main function is to liberate snR190 and U14 from each other. Rnt1 cleavage also removes the TMG cap from the precursor transcript, exposing it to the 5′→3′ exonucleases. The next step consists of the trimming of the remaining 5′ and the 3′ extensions by exonucleases (Figure 4; Lafontaine and Tollervey, 1995; Petfalski *et al*., 1998). 5′→3′ exonucleolytic trimming of the 5′ extensions of U14 and snR190 is due to the action of two exonucleases, Rat1 and Xrn1 (Petfalski *et al*., 1998). It is significant that yeast cells debilitated for Rat1 and Xrn1 accumulate 5′-extended species of snR190 and U14 whose 5′ ends are identical to the ends generated by Rnt1 cleavage (Lafontaine and Tollervey, 1995; Petfalski *et al*., 1998). The activity which removes the 3′ extensions is still unknown; the availability of the *rna82* mutant which accumulates 3′-extended species may lead to the identification of one of these activities (Lafontaine and Tollervey, 1995). Given the involvement of exonucleases in the processing pathway, the important stability of the UMO1 and UMO3 RNAs *in vivo* (Figure 2B) may be explained by the fact that both contain the same 5′ extension which is TMG-capped at its 5′ end (Figure 2C). In contrast, the UMO2 is much less abundant, probably because it does not contain this extension and is therefore much more vulnerable to exonucleases. Finally, it is worth noting that low levels of mature snR190, and to a lesser extent of U14 snoRNA, are still present in the context of the *RNT1* disruption. This suggests that exonucleases can partially overcome the requirement for Rnt1 to yield mature snoRNAs, or that there is another RNA endonuclease that can cleave the dicistronic substrate inefficiently.

### *Is the snR190–U14 cistron an intronic fossil?*

Genes encoding snoRNAs are usually classified into two families: snoRNAs which are encoded within introns, and independent transcriptions units, which are monocistronic, or polycistronic as in plants. At first glance, the snR190–U14 cistron seems to be a particular case of an independent transcription unit. However, we have noticed within the snR190–U14 region intriguing sequence similarities to intron-specific sequences. A pseudo 5′ splice site is present 10 nucleotides downstream from the 5′ end of the dicistronic precursor (GTAaTGT instead of GTATGT). A pseudo branch site sequence (TACcAAC instead of TACTAAC) is present 42 nucleotides downstream from the U14 coding sequence, followed by a polypyrimidine-rich tract and a 3′ splice site CAG. However, no potential ORF is present in the sequences upstream and downstream of these sequences. The same observation of degenerated splice sites without neighboring ORFs was made in *Schizosaccharomyces pombe*, where U14 appears to be encoded independently of snR190 (Samarsky *et al*., 1996). In vertebrates, U14 is encoded within introns of the *hsc70* gene (Leverette *et al*., 1992; Barbhaiya *et al*., 1994). It is possible that in the past, yeast U14 was encoded within an intronic sequence, and that this intron was inactivated

more or less recently by mutations. In yeast, single mutations within highly conserved intronic sequences usually have dramatic effects on splicing efficiency of intron-containing transcripts (see, for example, Vijayraghavan *et al*., 1986). This inactivation would not necessarily perturb the processing of the encoded snoRNAs because an endonucleolytic cleavage has been observed in some cases of processing of intron-encoded snoRNAs out of unspliced pre-mRNAs (Leverette *et al*., 1992; Caffarelli *et al*., 1994). Thus it is possible that some transitions may exist between the two families of genes encoding snoRNAs, the intron-encoded snoRNAs and the independent transcription units. Partial sequences of U14 from closely related yeast species have been published (Samarsky *et al*., 1996), but the full sequences of the corresponding genes are not available. If the hypothesis of an intronic molecular fossil is true and if inactivation of this intron is a recent event, identification of the complete genes encoding snR190 and U14 in closely related yeast species would be highly informative.

Whatever the origin of the genomic organization of the snR190–U14 cistron, this organization is not unique, because snoRNA polycistronic units have been described in plants (Leader *et al*., 1994, 1997). In that case, processing of these polycistronic transcripts probably requires an endonucleolytic cleavage event (Leader *et al*., 1997). An RNase III-like ORF is present in *Caenorhabditis elegans* (Rotondo and Frendewey, 1996), and we have found mouse and human expressed sequence tags in databases with sequence similarity to RNase III (data not shown). No RNase III-like sequence is known in plants, but since ortholog ORFs are present in *S.cerevisiae*, *S.pombe* (Rotondo and Frendewey, 1996) and metazoans, it seems likely that RNase III activity is present among very different eukaryotes and that one or several RNase III-like ORFs will soon be identified on sequencing plant genomes. If this prediction is correct, it seems likely that processing of some of the polycistronic plant transcripts will depend on such an activity.

## Materials and methods

### *Oligonucleotides, plasmids and probes*

Oligonucleotide probes used in this study were (5′→3′): U14, ACGATGGGTTCGTAAGCGTACTCCTACCGTGG; snR190, GGCTCAGATCTGCATGTGTTG; Seq190, CATGGTCGAATCGGACGAGG; UPS, GTGCAATGCTGAAGTCGAAAGAGGAGG; ITS, ATCTGTCTCCTCAAATTACCCAC; UPSb, GTGTCATGAAATTTCTCTTGAGATTATTCAAAC. They were prepared by kinasing 10–20 pmol of crude oligonucleotides with 25–50 μCi of [γ-$^{32}$P]ATP in a 10 μl reaction [70 mM Tris–HCl pH 7.6, 10 mM $MgCl_2$, 5 mM dithiothreitol (DTT), 10 U of T4 polynucleotide kinase from New England Biolabs]. The reaction was incubated for 30 min at 37°C, and for 5 min at 85°C to inactivate the kinase, and was run through two G-25 Microspin spin columns (Pharmacia) to remove unincorporated label.

Plasmids encoding the antisense probes or the substrate for *in vitro* cleavage assays were all generated using the same strategy. A PCR fragment was generated with *Pfu* polymerase (Stratagene) with a forward primer carrying a T7 promoter. The PCR product was cloned into PSP64 which carries an SP6 promoter (Krieg and Melton, 1987). Thus, using appropriate digestion, the same plasmid can be used for *in vitro* transcription with SP6 RNA polymerase to obtain antisense probes or with T7 RNA polymerase to obtain substrates for *in vitro* cleavage assays. Details of the constructs are available upon request. *In vitro* transcription was performed with linearized plasmid templates, as described (Chanfreau and Jacquier, 1996), except that [α-$^{33}$P]UTP was used for labeling. Transcripts were not capped.

### *RNT1 disruption*

Standard genetic and microbiological methods were used (Guthrie and Fink, 1991). The *S.cerevisiae* strain used for *RNT1* disruption is the diploid strain BMA64 (Baudin-Baillieu *et al*., 1997) which is derived from W303: *MATa/α*; *ura3-1/ura3-1*; *Δtrp1/Δtrp1*; *ade2-1/ade2-1*; *leu2-3,112/leu2-3,112*; *his3-11,15/his 3-11,15*. Disruption was done using a PCR strategy, as described in Baudin *et al*. (1993), resulting in the replacement of the complete ORF by the *TRP1* auxotrophy marker. Oligonucleotides used for generating the PCR product for the disruption were: 5′ RNT1-TRP, gcgcatatagaagagagcaaaactgtcctatttacaagcttttcaaaacaGGCCAAGAGGGAGGGC; and 3′ RNT1-TRP, gctaaagaaaatcaatgcaagttccatcatggttgtgtaaaaggaacgttCTTAAATAAATACTACTC. Lower case letters correspond to the sequences of the recombination arms 5′ and 3′ to the *RNT1* gene. Upper case letters are sequences which prime on the *TRP1* auxotrophy marker. Successful disruption was confirmed by Southern blot and PCR analysis. The stability of the *RNT1* disruption in the slow-growing spores was confirmed by PCR.

### *RNA extraction and Northern blotting*

We harvested 50–100 ml of wild-type or *rnt1Δ* sister spores cells in mid-log phase ($OD_{600}$ 0.15–0.5) washed them once in water, transferred them to 2 ml screw-cap Eppendorf tubes and stored them frozen at –80°C. Cells were resuspended in 200 μl of RNA buffer (50 mM Tris–HCl pH 7.5, 100 mM NaCl, 10 mM EDTA pH 8.0). Then 300–500 μl of acid-washed glass beads (425–600 μm diameter) were added, and the tubes were vortexed twice for 1 min, with 2 min on ice in between. Aliquots (200 μl) of RNA buffer, 10% SDS (50 μl) and acid phenol/chloroform/isoamylic acid (50/49/1) (400 μl) were added. The tubes were vortexed for 1 min and incubated for 10 min at 65°C. After phenol–choloroform extraction, the RNAs were extracted twice more with phenol–chloroform, precipitated with ethanol/sodium acetate (95%/100 mM), washed with 80% ethanol (v/v) and resuspended in distilled water.

For Northern blotting, 5–10 μg of total RNAs were denatured for 5 min at 85°C in formamide loading buffer (FLB: 95% deionized formamide, 40 mM EDTA pH 8.0, 0.05% xylene cyanol, 0.05% bromophenol blue), and loaded on a 5% polyacrylamide sequencing gel. After the run, RNAs were blotted onto nylon membranes (N+, Amersham) by semi-dry blotting in 0.5× TBE using a Biorad Transblot SD apparatus (1 h, 1.5 A, 5–15 V). The membrane was cross-linked with UV, pre-hybridized for 10–30 min in 5–15 ml of Rapid Hybridization Buffer (Amersham), and hybridized for 1 h at 42°C with 10–20 pmol of 5′ end-labeled oligonucleotide probes (see above). Membranes were washed at room temperature twice for 15 min with 2× SSPE, 0.1% SDS and once for 15 min with 0.2× SSPE, 0.1% SDS. Membranes were exposed on a PhosphorImager or a few hours for autoradiography with Biomax films (Kodak) without intensifying screens. Membrane stripping was done at 65°C for 1 h in 0.1% SDS or in 0.1× SSPE, 0.1% SDS.

### *Immunoprecipitations*

Protein G–Sepharose (Pharmacia) was washed three times with IP buffer (50 mM Tris–HCl pH 7.5, 5 mM EDTA pH 8.0, 250 mM NaCl, 0.05% NP-40), and 40 μl of the slurry was incubated at 6°C for 1 h with nutation with 2 μg of monoclonal antibody 12CA5 (BabCo) or monoclonal antibody K121 (Oncogene Research) which recognizes TMG caps. After antibody binding, beads were washed three times with IP buffer. Twenty μl of each slurry was incubated for 2 h at 6°C with 10–20 μg of total RNAs extracted from wild-type or *rnt1Δ* strains. Beads were washed five times with IP buffer, and total RNAs were extracted by digestion with 10 μg of proteinase K and phenol–chloroform extraction. Northern blot analysis of immunoprecipitated RNAs was as above.

### *Primer extension*

Total RNAs (2–4 μg) were denatured for 3 min at 85°C in the presence of 0.3 pmol of 5′-labeled oligonucleotide in a total volume of 2.5 μl and incubated for 5 min at 45°C. Elongation was done for 25 min at 45°C in a 5 μl reaction [50 mM Tris pH 8.3, 75 mM KCl, 3 mM $MgCl_2$, 10 mM DTT, 0.05 μg/μl actinomycin D, 500 μM dNTPs and 20 U/μl Mo-MLV reverse transcriptase (Gibco-BRL)]. Reactions were stopped by addition of 5 μl of FLB, denatured for 5 min at 85°C and loaded on 5% sequencing gels. To obtain a sequencing ladder, half of a standard 50 μl PCR reaction was denatured for 5 min at 100°C with 2 pmol of 5′-labeled oligonucleotide and chilled on ice; extension was done using Sequenase reagents (USB) without labeling mix.

### *RNase A/T1 mapping*

$^{33}$P-labeled probes for RNase protection were obtained by *in vitro* transcription of the corresponding linearized plasmids, as described (Chanfreau and Jacquier, 1996). Total RNAs (2–4 µg) were denatured for 10 min at 85°C with 50 fmol of gel-purified $^{33}$P internally labeled RNA probe, in 80% deionized formamide, 40 mM PIPES pH 6.5, 400 mM NaCl, 1 mM EDTA. Annealing was performed for 4 h at 45°C in 30 µl. Digestion was done by addition of 270 µl of digestion cocktail (1 µg RNase A; 500 U of RNase T1 from Boehringer Mannheim; 10 mM Tris–HCl pH 7.5; 300 mM NaCl; 5 mM EDTA) for 30 min at 37°C. Reactions were stopped by adding 7.5 µl of 20% SDS and 10 µg of proteinase K. RNAs were extracted by phenol–chloroform, precipitated with ethanol, resuspended in FLB and loaded on 5 or 6% sequencing gels.

### *In vitro processing reactions*

Whole-cell extracts were prepared from wild-type and *rnt1*Δ sister spore strains as described (Umen and Guthrie, 1995). For the chase experiment of Figure 4, 10 µl reactions included 3 µl of whole-cell extract, 60 mM potassium phosphate (pH 7.2), 3% polyethyleneglycol (PEG; average mol. wt 8000), 10 mM $MgCl_2$ and 0.5 µg/µl wheat-germ tRNA, and were incubated for 45 min at 30°C with buffer alone or with 3 pmol of GST–Rnt1 or 100 pmol of GST, prepared as described (Abou Elela *et al*., 1996) from an *E.coli* strain lacking the *rnc* gene encoding RNase III (kind gift of A.Nicholson). Reactions were stopped with 300 µl of STOP buffer (Chanfreau *et al*., 1997) with 10 µg of proteinase K and 20 µg of glycogen as a carrier. RNAs were extracted with phenol–chloroform, precipitated with ethanol and loaded on a 5% acrylamide sequencing gel. Northern blotting was as described above. For *in vitro* cleavage of the *in vitro* synthesized transcripts, 0.1 pmol of gel-purified $^{33}$P-labeled dicistronic substrate was incubated for the time indicated at 24°C in 5 µl reactions (30 mM KCl, 10 mM $MgCl_2$, 30 mM Tris–HCl pH 7.5, 0.1 mM DTT, 0.1 mM EDTA, 0.5µg/µl wheat-germ tRNA) with 10–40 pmol of GST or 0.1–0.3 pmol of GST–Rnt1. Reactions were quenched by addition of 5 µl of FLB and directly loaded on a 5% sequencing gel after 3 min of denaturation at 100°C. Cleavage in extracts was done for 2.5 min in 60 mM potassium phosphate (pH 7.2), 3% PEG (average mol. wt 8000) and 10 mM $MgCl_2$, and RNAs were extracted as above. For RNase H mapping, 10–100 fmol of the gel-purified fragments were denatured for 5 min at 85°C with 10 pmol of the corresponding oligonucleotides and 5 µg of wheat-germ tRNA in 2.5 µl. Annealing was done for 20 min at 37°C. RNase H digestion was done in 5 µl of 40 mM Tris–HCl pH 7.5, 50 mM KCl, 5 mM $MgCl_2$, 1 U of *E.coli* RNase H (from USB) for 30 min at 37°C. Reactions were stopped by addition of 5 µl of FLB and loaded on sequencing gels. Primer extension analysis of the cleavage fragments was done as above.

## Acknowledgements

We thank C.Coffinier, M.Fromont, D.Lallemand, J.-C.Rain and C.Transy for suggestions and technical advice, B.Dujon's lab for extensive use of their hybridization equipment, S.Noble for the gift of oligonucleotides, M.Ares for the RNT1 and GST–RNT1 plasmids, A.Nicholson for the RNase III$^-$ *E.coli* strain, M.Ares and D.Tollervey for sharing results prior to publication, and M.Ares, C.Coffinier, E.Fabre, J.Staley and D.Tollervey for critical reading of the manuscript. G.R was supported by a fellowship from the EEC (Human Capital and Mobility). G.C. is chargé de recherches at the CNRS.

## References

Abou Elela,S. and Ares,M., Jr (1998) Depletion of yeast RNase III blocks correct U2 3′ end formation and results in polyadenylated but functional U2 snRNA. *EMBO J.*, **17**, 3738–3746.

Abou Elela,S., Igel,H. and Ares,M.,Jr (1996) RNase III cleaves eukaryotic preribosomal RNA at a U3 snoRNP-dependent site. *Cell*, **85**, 115–124.

Bachellerie,J.P., Michot,B., Nicoloso,M., Balakin,A., Ni,J. and Fournier, M.J. (1995) Antisense snoRNAs: a family of nucleolar RNAs with long complementarities to rRNA. *Trends Biochem. Sci.*, **20**, 261–264.

Balakin,A.G., Lempicki,R.A., Huang,G.M. and Fournier,M.J. (1994) *Saccharomyces cerevisiae* U14 small nuclear RNA has little secondary structure and appears to be produced by post-transcriptional processing. *J. Biol. Chem.*, **269**, 739–746.

Balakin,A.G., Smith,L. and Fournier,M.J. (1996) The RNA world of the nucleolus: two major families of small RNAs defined by different box elements with related functions. *Cell*, **86**, 823–834.

Barbhaiya,H., Leverette,R.D., Liu,J. and Maxwell,E.S. (1994) Processing of U14 small nucleolar RNA from three different introns of the mouse 70-kDa-cognate-heat-shock-protein pre-messenger RNA. *Eur. J. Biochem.*, **226**, 765–771.

Baudin,A., Ozier-Kalogeropoulos,O., Denouel,A., Lacroute,F. and Cullin,C. (1993) A simple and efficient method for direct gene deletion in *Saccharomyces cerevisiae*. *Nucleic Acids Res.*, **21**, 3329–3330.

Baudin-Baillieu,A., Guillemet,E., Cullin,C. and Lacroute,F. (1997) Construction of a yeast strain deleted for the TRP1 promoter and coding region that enhances the efficiency of the polymerase chain reaction-disruption method. *Yeast*, **13**, 353–356.

Caffarelli,E., Arese,M., Santoro,B., Fragapane,P. and Bozzoni,I. (1994) *In vitro* study of processing of the intron-encoded U16 small nucleolar RNA in *Xenopus laevis*. *Mol. Cell. Biol.*, **14**, 2966–2974.

Caffarelli,E., Fatica,A., Prislei,S., De Gregorio,E., Fragapane,P. and Bozzoni,I. (1996) Processing of the intron-encoded U16 and U18 snoRNAs: the conserved C and D boxes control both the processing reaction and the stability of the mature snoRNA. *EMBO J.*, **15**, 1121–1131.

Cavaille,J., Nicoloso,M. and Bachellerie,J.P. (1996) Targeted ribose methylation of RNA *in vivo* directed by tailored antisense RNA guides. *Nature*, **383**, 732–735.

Chanfreau,G. and Jacquier,A. (1996) An RNA conformational change between the two chemical steps of group II self-splicing. *EMBO J.*, **15**, 3466–3476.

Chanfreau,G., Abou Elela,S., Ares,M.,Jr and Guthrie,C. (1997) Alternative 3′ end processing of U5 snRNA by RNase III. *Genes Dev.*, **11**, 2741–2751.

Chelladurai,B., Li,H., Zhang,K. and Nicholson,A.W. (1993) Mutational analysis of a ribonuclease III processing signal. *Biochemistry*, **32**, 7549–7558.

Court,D. (1993) RNase III: A double strand processing enzyme. In Brawerman,G. and Belasco J. (eds), *Control of Messenger RNA Stability.* Academic Press, New York, pp. 70–116.

Dichtl,B., Stevens,A. and Tollervey,D. (1997) Lithium toxicity in yeast is due to the inhibition of RNA processing enzymes. *EMBO J.*, **16**, 7184–7195.

Fragapane,P., Prislei,S., Michienzi,A., Caffarelli,E. and Bozzoni,I. (1993) A novel small nucleolar RNA (U16) is encoded inside a ribosomal protein intron and originates by processing of the pre-mRNA. *EMBO J.*, **12**, 2921–2928.

Ganot,P., Bortolin,M.L. and Kiss,T. (1997a) Site-specific pseudouridine formation in preribosomal RNA is guided by small nucleolar RNAs. *Cell*, **89**, 799–809.

Ganot,P., Caizergues-Ferrer,M. and Kiss,T. (1997b) The family of box ACA small nucleolar RNAs is defined by an evolutionarily conserved secondary structure and ubiquitous sequence elements essential for RNA accumulation. *Genes Dev.*, **11**, 941–956.

Guthrie,C. and Fink,G.R. (1991) *Guide to Yeast Genetics and Molecular Biology.* Academic Press, San Diego, CA.

Huang,G.M., Jarmolowski,A., Struck,J.C. and Fournier,M.J. (1992) Accumulation of U14 small nuclear RNA in *Saccharomyces cerevisiae* requires box C, box D and a 5′, 3′ terminal stem. *Mol. Cell. Biol.*, **12**, 4456–4463.

Kiss,T. and Filipowicz,W. (1993) Small nucleolar RNAs encoded by introns of the human cell cycle regulatory gene *RCC1*. *EMBO J.*, **12**, 2913–2920.

Kiss,T. and Filipowicz,W. (1995) Exonucleolytic processing of small nucleolar RNAs from pre-mRNA introns. *Genes Dev.*, **9**, 1411–1424.

Kiss-Laszlo,Z., Henry,Y., Bachellerie,J.P., Caizergues-Ferrer,M. and Kiss,T. (1996) Site-specific ribose methylation of preribosomal RNA: a novel function for small nucleolar RNAs. *Cell*, **85**, 1077–1088.

Krainer,A.R. (1988) Pre-mRNA splicing by complementation with purified human U1, U2, U4/U6 and U5 snRNPs. *Nucleic Acids Res.*, **16**, 9415–9429.

Krieg,P.A. and Melton,D.A. (1987) *In vitro* RNA synthesis with SP6 RNA polymerase. *Methods Enzymol.*, **155**, 397–415.

Lafontaine,D. and Tollervey,D. (1995) Trans-acting factors in yeast pre-rRNA and pre-snoRNA processing. *Biochem. Cell. Biol.*, **73**, 803–812.

Leader,D.J., Sanders,J.F., Waugh,R., Shaw,P. and Brown,J.W. (1994) Molecular characterisation of plant U14 small nucleolar RNA genes: closely linked genes are transcribed as polycistronic U14 transcripts. *Nucleic Acids Res.*, **22**, 5196–5203.

Leader,D.J., Clark,G.P., Watters,J., Beven,A.F., Shaw,P.J. and Brown,J.W. (1997) Clusters of multiple different small nucleolar RNA genes in plants are expressed as and processed from polycistronic pre-snoRNAs. *EMBO J.*, **16**, 5742–5751.

Leverette,R.D., Andrews,M.T. and Maxwell,E.S. (1992) Mouse U14 snRNA is a processed intron of the cognate hsc70 heat shock pre-messenger RNA. *Cell*, **71**, 1215–1221.

Li,H.D., Zagorski,J. and Fournier,M.J. (1990) Depletion of U14 small nuclear RNA (snR128) disrupts production of 18S rRNA in *Saccharomyces cerevisiae*. *Mol. Cell. Biol.*, **10**, 1145–1152.

Liang,W.Q. and Fournier,M.J. (1995) U14 base-pairs with 18S rRNA: a novel snoRNA interaction required for rRNA processing. *Genes Dev.*, **9**, 2433–2443.

Liu,J. and Maxwell,E.S. (1990) Mouse U14 snRNA is encoded in an intron of the mouse cognate hsc70 heat shock gene. *Nucleic Acids Res.*, **18**, 6565–6571.

Maxwell,E.S. and Fournier,M.J. (1995) The small nucleolar RNAs. *Annu. Rev. Biochem.*, **64**, 897–934.

Morrissey,J.P. and Tollervey,D. (1997) U14 small nucleolar RNA makes multiple contacts with the pre-ribosomal RNA. *Chromosoma*, **105**, 515–522.

Ni,J., Tien,A.L. and Fournier,M.J. (1997) Small nucleolar RNAs direct site-specific synthesis of pseudouridine in ribosomal RNA. *Cell*, **89**, 565–573.

Petfalski,E., Dandekar,T., Henry,Y. and Tollervey (1998) Processing of precursors to small nucleolar RNAs and ribosomal RNAs requires common components. *Mol. Cell. Biol.*, **18**, 1181–1189.

Prislei,S., Michienzi,A., Presutti,C., Fragapane,P. and Bozzoni,I. (1993) Two different snoRNAs are encoded in introns of amphibian and human L1 ribosomal protein genes. *Nucleic Acids Res.*, **21**, 5824–5830.

Rotondo,G. and Frendewey,D. (1996) Purification and characterization of the Pac1 ribonuclease of *Schizosaccharomyces pombe*. *Nucleic Acids Res.*, **24**, 2377–2386.

Samarsky,D.A., Schneider,G.S. and Fournier,M.J. (1996) An essential domain in *Saccharomyces cerevisiae* U14 snoRNA is absent in vertebrates, but conserved in other yeasts. *Nucleic Acids Res.*, **24**, 2059–2066.

Smith,C.M. and Steitz,J.A. (1997) Sno storm in the nucleolus: new roles for myriad small RNPs. *Cell*, **89**, 669–672.

Takiff,H.E., Chen,S.M. and Court,D.L. (1989) Genetic analysis of the *rnc* operon of *Escherichia coli*. *J. Bacteriol.*, **171**, 2581–2590.

Tollervey,D. (1996) Small nucleolar RNAs guide ribosomal RNA methylation. *Science*, **273**, 1056–1057.

Tollervey,D. and Kiss,T. (1997) Function and synthesis of small nucleolar RNAs. *Curr. Opin. Cell Biol.*, **9**, 337–342.

Tycowski,K.T., Shu,M.D. and Steitz,J.A. (1993) A small nucleolar RNA is processed from an intron of the human gene encoding ribosomal protein S3. *Genes Dev.*, **7**, 1176–1190.

Tycowski,K.T., Shu,M.D. and Steitz,J.A. (1996a) A mammalian gene with introns instead of exons generating stable RNA products. *Nature*, **379**, 464–466.

Tycowski,K.T., Smith,C.M., Shu,M.D. and Steitz,J.A. (1996b) A small nucleolar RNA requirement for site-specific ribose methylation of rRNA in *Xenopus*. *Proc. Natl Acad. Sci. USA*, **93**, 14480–14485.

Umen,J.G. and Guthrie,C. (1995) A novel role for a U5 snRNP protein in 3′ splice site selection. *Genes Dev.*, **9**, 855–868.

Vijayraghavan,U., Parker,R., Tamm,J., Iimura,Y., Rossi,J., Abelson,J. and Guthrie,C. (1986) Mutations in conserved intron sequences affect multiple steps in the yeast splicing pathway, particularly assembly of the spliceosome. *EMBO J.*, **5**, 1683–1695.

Watkins,N.J., Leverette,R.D., Xia,L., Andrews,M.T. and Maxwell,E.S. (1996) Elements essential for processing intronic U14 snoRNA are located at the termini of the mature snoRNA sequence and include conserved nucleotide boxes C and D. *RNA*, **2**, 118–133.

Xia,L., Watkins,N.J. and Maxwell,E.S. (1997) Identification of specific nucleotide sequences and structural elements required for intronic U14 snoRNA processing. *RNA*, **3**, 17–26.

Yoo,C.J. and Wolin,S.L. (1997) The yeast La protein is required for the 3′ endonucleolytic cleavage that matures tRNA precursors. *Cell*, **89**, 393–402.

Zagorski,J., Tollervey,D. and Fournier,M.J. (1988) Characterization of an SNR gene locus in *Saccharomyces cerevisiae* that specifies both dispensible and essential small nuclear RNAs. *Mol. Cell. Biol.*, **8**, 3282–3290.

Zhang,K. and Nicholson,A.W. (1997) Regulation of ribonuclease III processing by double-helical sequence antideterminants. *Proc. Natl Acad. Sci. USA*, **94**, 13437–13441.

Zuker,M. (1994) Prediction of RNA secondary structure by energy minimization. *Methods Mol. Biol.*, **25**, 267–294.

*Received March 11, 1998; revised May 6, 1998; accepted May 7, 1998*